Available online at www.elixirpublishers.com (Elixir International Journal)

Computational Chemistry

Elixir Comp. Chem. 63 (2013) 18536-18554

ISSN: 2229-712X

# Experimental and theoretical investigations of spectroscopic properties of N-acetyl thiourea

R.Kumutha[1], M.Thirumalai Kumar[2] and S.Sampath Krishnan[3,*]

[1]Department of Physics, Jaya Engineering College, Thiruninravur, Chennai -602 024, India.

[2]Department of Applied Chemistry, Sri Venkateswara College of Engineering, Sriperumbudur-602 105, India.

[3]Department of Applied Physics, Sri Venkateswara College of Engineering, Sriperumbudur-602 105, India.

**ARTICLE INFO**

**Article history:**

Received: 22 June 2013;

Received in revised form:

29 September 2013;

Accepted: 16 October 2013;

**Keywords**

Normal coordinate analysis,

FT-IR & FT-Raman spectrum,

N-acetyl Thiourea.

**ABSTRACT**

The Fourier transform infrared (FT-IR) spectra and FT-Raman spectra of N –acetyl thiourea (NATU) was recorded in the regions 4000-400 $cm^{-1}$ respectively, in the solid phase. Molecular electronic energy, geometrical structure, harmonic vibrational frequencies and bonding features of the title compound were computed three parameter hybrid functional Lee-Yang –Parr/6-31G(d,p) and 6-311++G(d,p) levels of theory. The vibrational studies were interpreted in terms of potential energy distribution. The results were compared with experimental values with the help of harmonic vibrational spectra. Infrared intensities and Raman scattering activities, highest occupied molecular orbital, lowest unoccupied molecular orbital energy, and energy gaps were computed above method. The observed wave number in FTIR spectra was analyzed and assigned to different normal modes of the molecule. Most of the modes have wave numbers in the expected range and are in good agreement with computed values. The first order hyperpolarizability of this molecular system and related properties (β, μ, α and Δα) are calculated using B3LYP method based on the finite-field approach. Stability of the molecule arising from hyper conjugative interactions, charge delocalization and intermolecular hydrogen bond-like weak interaction has been analyzed using natural bond orbital (NBO) analysis by using B3LYP method. The results show that electron density (ED) in the σ* and π*antibonding orbital's and second-order delocalization energies $E^{(2)}$ confirm the occurrence of intra-molecular charge transfer (ICT) within the molecule.



## Introduction

DFT methods are increasingly applied to representative pharmacological compounds aiming to elucidate their molecular structures, electronic properties and bonds, the establishment of electronic and structural factors of selected reactions and their mechanisms. These studies contribute to the recognition of structure-activity relationships and to the understanding of the properties and system behavior. For a proper understanding of IR and Raman spectra, a reliable assignment of all vibrational bands is essential. For this purpose, the quantum chemical methods, ranging from semi-empirical to DFT approaches, are invaluable tools[1,3], each method having its own advantages. The semi empirical calculations provide very fast, and in certain circumstances fairly good theoretical results, being applicable to large molecular systems. The Hartree-Fock *Ab Initio* methods are able to give good results provided a reasonable basis set and an appropriate correlation treatment is taken into account. On the other hand, DFT methods, particularly hybrid functional methods [4], have evolved to a powerful quantum chemical tool for the determination of the electronic structure of molecules. In the framework of DFT approach, different exchange and correlation functional are routinely used. Among these, the B3LYP combination [5,6] is the most used since it proved its ability in reproducing various molecular properties, including vibrational spectra. The combined use of B3LYP functional and standard split valence basis set 6-311G(d) has been previously shown[7,9] to provide an excellent compromise between accuracy and computational efficiency of vibrational spectra for large and medium-size molecules.

Thiourea is an organic compound of carbon, nitrogen, sulfur and hydrogen with the formula $(NH_2)_2CS$. This compound is important for the study of spectroscopic structural and ligational proprieties. This compound is one of the simplest molecular C=S moiety is a part of a conjugated system involving a $\pi$ - lone pairs of planar amine nitrogen. It also provides in appropriate model for

Tele:

E-mail addresses: sambathk@svce.ac.in

the study of properties of S=C-C-NH group. A fundamental building block in the chemical skeleton of thiopurines and thiopyrimidines which are found to occur as minor components of the structure of TRNA [11,12]. Thiopurines and thiopyrimidines differs from the natural bases of the nucleic acid only by a substitution of the thiocarbonyl for the carbonyl double bond. Moreover most of these sulfur nitrogen compounds like thiourea containing NHCSNH2 skeleton have been found to possess carcinstatic and antiviral activities [13]. It is of interest to study the spectral and structural feature of N- acetylthiourea. Acetylthiourea is isoelectronic with monothiobiuret and is the sulfur analog of N- acetyl urea for both of which detailed vibration studies have been done recently[14,15]. A complete normal coordinate analysis has been carried out N – acetylthiourea using an intramolecular potential field of the Urey- bardley type supplemented with valence force function for the Out- of plane modes. The assignments made for N-acetylthiourea for discussed in comparison with related molecules.

**Computational Method**

The DFT Computation of N acetyl thiourea has been performed using Gaussian 03 program package[16] at the Becke3-Lee-Yang –Parr (B3LYP) level with standard 6.311G(d,p) and 6-311++G(d,p) basic sets. The geometries were optimized without any constraint with the help of analytical gradient procedure implemented within Gaussian 03 program. The harmonic vibrational wave number have been analytically calculated by taking the second derivative of energy using the simple level of theory. Multiple scaling of the force field was performed y SQM procedure [17,18] to offset the systematic errors caused by basis set incompleteness, neglect of electron correlation and vibrational anharmonicity Normal coordinate analysis has been performed to obtain full description of the molecular motion pertaining to the normal modes with MOLVIB Program version 7.0 written by Sundius[19,20]. For plots of simulated IR spectra, pure Lorentizian band shapes were used with a bandwidth (FWHM) of 10 $cm^{-1}$ .The Raman intensities (Si) calculated by Gaussian 03 program have been suitably adjusted by the scaling procedure with MOLVIB and subsequently converted to relative Raman intensities ($I_i$) using the following relationship derived from the basis theory of Raman Scattering[21,22]

$$I_i = \frac{f(\nu_o - \nu_i)^4 S_i}{\nu_i \left[1 - \exp\left(\frac{-hcr_i}{kt}\right)\right]}$$

Where $\gamma_o$ is the exciting frequency (in $cm^{-1}$ units) $\gamma_i$ is the vibrational wave number of the $i^{th}$ mode, h, c, k are universal constants, and f is suitably chosen common scaling factor for all the peak intensities. The stimulated IR and Raman have been plotted using the Lorentizian shape with full width at half maximum (FWHM) of 10 $Cm^{-1}$. Natural bond (NBO) analysis has been performed using NBO 3.1 program as implemented in the Gaussian 03 W package at the DFTB3LYP/6.311++G level of theory

**Potential energy distribution**

In the normal coordinate analysis by Wilson's GF matrix method[23]. It is possible to obtain useful information about the fundamental vibrational modes from the *L* matrix whose columns are the characteristic vectors of the *GF* matrix. The *L* matrix is given by the internal symmetry coordinate matrix *R* and the normal coordinate matrix *Q* as

*R=LQ.*

The potential energy *V* for the normal vibration associated with normal coordinate $Q_k$ can bewritten in the form

$$V = \frac{1}{2}\sum_{i,j} F_{ij} R_i R_J = \frac{1}{2}\sum_k Q_k^2 \sum_{i,j} F_{ij} L_{jk} L_{ik}$$

where $R_i$ is the internal coordinates and $F_{ij}$ are the force constants. The quantities $L_{ik}$ are the elements of the matrix of the vibrational modes *L* (the transformation matrix).If the force constant matrix is known, one can compute $L_{jk}$ *Lik* $F_{ij}$ terms, and obtained a two-dimensional, symmetric matrix of these terms for each normal coordinate [24,25] Instead of these matrices, however, usually a single potential energy distribution matrix, PED, is applied, whose elements are given by

$$\left[PED\right]_{kj} = \sum_i L_{jk} L_{ik} F_{ij}$$

Some authors prefer normalizing the matrix elements with respect to the calculated eigenvalues,

$\lambda_k$, to obtain

$$\left[PED\right]_{kj}^{\lambda} = \frac{\sum_i L_{jk} L_{ik} F_{ij}}{\lambda_k}$$

The distribution of potential energy in each internal coordinate is of great help in assigning the calculated vibrations of molecules. In many cases this distribution permits frequencies to be assigned to specific vibrations more reliably than the modes of vibration themselves

**The global quantities**

In DFT, the ground state energy of an atom or a molecule in terms of its electron density ρ(r) is written as [26]

$$E[\rho] = F[\rho] + \int dr v(r)\ \rho\ (r) \qquad (1)$$

where v(r) is the external potential that includes the nuclear potential also, and F[ $\rho$ is the universal Hohenberg - Kohn functional composed of the electronic kinetic energy and the electron-electron repulsion energy. The first and second partial derivatives of E[ $\rho$ ] with respect to the number of electron N under the constant external potential v(r) are defined as the chemical potential $\mu$, electronegativity ($\chi$), and the global hardness $\eta$ of the system respectively [27]

$$\mu = \left(\frac{\partial E}{\partial N}\right)_{V(r)} \qquad (2)$$

$$\eta = \frac{1}{2}\left(\frac{\partial^2 E}{\partial N^2}\right)_{V(r)} \qquad (3)$$

The inverse of the hardness is expressed as the global softness

$$S = \frac{1}{2}\eta \qquad (4)$$

The global descriptor of hardness has been an indicator of overall stability of the system. It has been customary to use a finite difference approximation for $\mu$ and $\eta$. Using the energies of N, (N+1) and (N-1) electron systems, we get the operational definition of $\mu$ and $\eta$ as [4],

$$\mu \approx -(IP + EA)/2 \qquad (5)$$

$$\eta \approx (IP - EA)/2 \qquad (6)$$

Where IP and EA are the first vertical ionization energy and electron affinity of the chemical species respectively

**Local Quantities:**

The site-selectivity of a chemical system, cannot, however, be studied using the global descriptors of reactivity. For this, appropriate local descriptors need be defined. An appropriate definition of local softness s(r) is given by [28],

$$S(r) = \left(\frac{\partial \rho(r)}{\partial \mu}\right)_{V(r)} \qquad (7)$$

Such that

$$\int s(r)dr = S$$

Combining Eqs. 7 and the definition of global softness, we can write

$$S(r) = \left(\frac{\partial \rho(r)}{\partial \mu}\right)_{V(r)} \qquad (8a)$$

$$S(r) = \left(\frac{\partial \rho(r)}{\partial \mu}\right)_{V(r)} \left(\frac{\partial N}{\partial \mu}\right)_{V(r)} \quad (8b)$$

$$= f(r)S \quad (8c)$$

where f(r) is defined as the Fukui function [29]. The Fukui function is defined as,

$$f(r) = \left(\frac{\partial \rho(r)}{\partial N}\right)_{V} = \left(\frac{\partial \mu}{\partial v(r)}\right)_{N} \quad (9)$$

The second relation can be obtained using the relation that density is the first partial derivative of

energy with respect to external potential at constant N. The Fukui function describes the sensitivity of the chemical potential of a system to a local external potential. Using left and right derivatives with respect to the number of electrons, electrophilic and nucleophilic Fukui function and local softness can be defined. To describe site selectivity or reactivity of an atom in a molecule, it is necessary to condense the values of f(r) and s(r) around each atomic site into a single value that characterizes the atom in a molecule. This can be achieved by electronic population analysis. Thus for an atom k in a molecule, depending upon the type of electron transfer, we have three different types of condensed Fukui function of the atom k,

$f_k+ = [qk\ (N+1) - qk\ (N)]$ for nucleophilic attack (10a)

$f_k- = [qk(N) - qk\ (N-1)]$ for electrophilic attack (10b)

$f_{k0} = [qk(N+1) - qk(N-1)]$ for radical attack (10c)

where qk is the gross electronic population of atom k in the molecule. The corresponding condensed local softness's sk+, sk- and sk0 can be defined. Parr and Yang proposed that larger value of Fukui function indicate more reactivity[28] Hence greater the value of the condensed Fukui function, the more reactive is the particular atomic center in the molecule. Subsequently, Gazquez and Mendez proposed a local version of HSAB principle, which generally states that the interaction between any two chemical species will occur through the centers with nearly equal condensed Fukui function[30,31]. This can determine the behavior of different reactive sites with respect to the hard and soft reagents.

**Result and Discussion**

**Normal Coordinate Analysis:**

Based on the result obtained by the Density Functional theory the molecules belonging to $C_S$ point group with 33 degree of freedom. The Gaussian molecular structure adopted for N-acetylthiourea is shown in Fig 1. The structural parameters, bond angle and bond distance are shown in Table 1. All the 33 fundamental vibrations are found to be both Infrared and Raman activities.

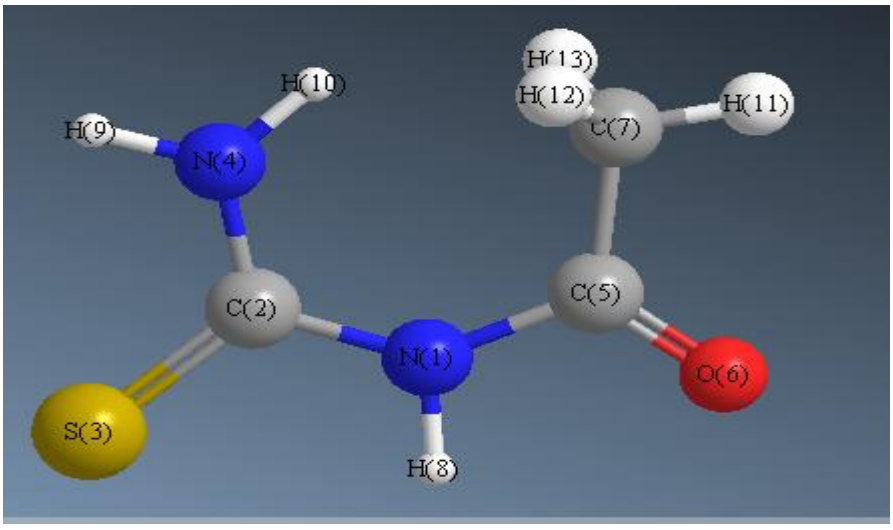


**Fig 1. Molecular structure and labeling of atoms in N-acetylthiourea**

**Vibrational Spectra analysis**

The vibrational spectral assignments have been carried out with the help of normal coordinate analysis. The Internal and Symmetry coordinator are presented in Table 2. In the harmonic vibration of frequency calculated for N-acetylthiourea at B3LYP levels using the triple split valence basis set 6-311++G(d,p) have been presented in Table 3, along with observed experimental data's. The relative values of IR intensity, Raman activity ,reduced mass, polarized and un-polarized along with force constants of B3LYP/6-311++G(d,p) of NATU is shown in Table 4. The comparison of the frequency calculated at B3LYP with experimental values reveals the overestimated of the calculated Vibrational mode, due to neglected of harmonicity in real systems. It is customize to scale down the calculated harmonic frequency in order to improve the agreement with the experiment. The frequency of stretching ($NH_2$, NH, & $CH_3$) where scaled by 0.96, the other harmonic frequencies below two thousands $cm^{-1}$, where scaled by the factor of 0.983, determine in the previous studies of similar organic systems.

**Table 1. Optimized geometrical parameters for NATU with different basis set.**

| PARAMETERS | EXPERIMENTAL | B3LYP/6-311G(d,p) | B3LYP/6-311++G(d,p) |
|---|---|---|---|
| **BOND LENGTH** | | | |
| C(7)-H(13) | 1.113 | 1.113 | 1.113 |
| C(7)-H(12) | 1.113 | 1.113 | 1.113 |
| C(7)-H(11) | 1.113 | 1.1129 | 1.1129 |
| N(4)-H(10) | 1.012 | 1.012 | 1.012 |
| N(4)-H(9) | 1.012 | 1.0121 | 1.0121 |
| N(1)-H(8) | 1.012 | 1.0121 | 1.0121 |
| N(1)-C(5) | 1.369 | 1.369 | 1.369 |
| C(5)-C(7) | 1.509 | 1.509 | 1.509 |
| C(5)-O(6) | 1.208 | 1.208 | 1.208 |
| C(2)-N(4) | 1.369 | 1.369 | 1.369 |
| C(2)-S(3) | 1.576 | 1.576 | 1.576 |
| N(1)-C(2) | 1.369 | 1.3689 | 1.3689 |
| **BOND ANGLE** | | | |
| H(13)-C(7)-H(12) | 109.52 | 109.5177 | 109.5177 |
| H(13)-C(7)-H(11) | 109.4618 | 109.4617 | 109.4617 |
| H(13)-C(7)-C(5) | 109.4618 | 109.4616 | 109.4616 |
| H(12)-C(7)-H(11) | 109.4418 | 109.4456 | 109.4456 |
| H(12)-C(7)-C(5) | 109.4418 | 109.4393 | 109.4393 |
| H(11)-C(7)-C(5) | 109.5 | 109.5014 | 109.5014 |
| N(1)-C(7)-C(5) | 120 | 120.0006 | 120.0006 |
| N(1)-C(5)-O(6) | 120 | 119.999 | 119.999 |
| C(7)-C(5)-O(6) | 120 | 120.0004 | 120.0004 |
| H(10)-N(4)-H(9) | 120 | 119.9977 | 119.9977 |
| H(10)-N(4)-C(2) | 120 | 119.9998 | 119.9998 |
| H(9)-N(4)-C(2) | 120 | 120.0026 | 120.0026 |
| N(4)-C(2)-S(3) | 120 | 119.9998 | 119.9998 |
| N(4)-C(2)-N(1) | 120 | 119.9984 | 119.9984 |
| S(3)-C(2)-N(1) | 120 | 120.0019 | 120.0019 |
| H(8)-N(1)-C(5) | 120 | 119.9977 | 119.9977 |
| H(8)-N(1)-C(2) | 120 | 120.0005 | 120.005 |
| C(5)-N(1)-C(2) | 120 | 120.0019 | 120.0019 |

**Table 2. Internal and symmetry coordinates for NATU**

| S.No | Symmetry Co-ordinates | Description* |
|---|---|---|
| 1 | $S_1 = \frac{1}{\sqrt{2}}(d_{11} - d_{12})$ | $\nu_a$ $NH_2$ |
| 2. | $S_2 = \frac{1}{\sqrt{2}}(d_{11} + d_{12})$ | $\nu_s$ $NH_2$ |
| 3. | $S_3 = d_7$ | $\nu$ NH |
| 4. | $S_4 = d_{10}$ | $\nu$ $CN$ |
| 5. | $S_5 = d_8$ | $\nu$ $CN'$ |
| 6. | $S_6 = d_6$ | $\nu$ $C'N'$ |
| 7. | $S_7 = d_9$ | $\nu$ $CS$ |
| 8. | $S_8 = d_1$ | $\nu$ $C'O$ |
| 9. | $S_9 = d_2$ | $\nu$ $CC'$ |
| 10. | $S_{10} = \frac{1}{\sqrt{3}}(d_3 + d_4 + d_5)$ | $\nu_s$ $CH_3$ |
| 11. | $S_{11} = \frac{1}{\sqrt{6}}(2d_5 - d_3 - d_4)$ | $\nu_a$ $CH_3$ |
| 12. | $S_{12} = \frac{1}{\sqrt{6}}(2\alpha_{11,12} - \alpha_{10,11} - \alpha_{10,12})$ | $\delta$ NH |
| 13. | $S_{13} = \frac{1}{\sqrt{2}}(\alpha_{10,12} - \alpha_{10,11})$ | $\rho$ $NH_2$ |
| 14. | $S_{14} = \frac{1}{\sqrt{2}}(\alpha_{8,9} - \alpha_{9,10})$ | $\delta$ CS |
| 15. | $S_{15} = \frac{1}{\sqrt{2}}(\alpha_{6,7} - \alpha_{7,8})$ | $\delta$ NH |
| 16. | $S_{16} = \frac{1}{\sqrt{6}}(2\alpha_{6,8} - \alpha_{6,7} - \alpha_{7,8})$ | $\delta$ C'N'C |
| 17. | $S_{17} = \frac{1}{\sqrt{2}}(\alpha_{6,2} - \alpha_{1,2})$ | $\delta$ CO |
| 18. | $S_{18} = \frac{1}{\sqrt{6}}(2\alpha_{1,6} - \alpha_{1,2} - \alpha_{6,2})$ | $\delta$ CC'N' |
| 19. | $S_{19} = \frac{1}{\sqrt{6}}(2\alpha_{10,8} - \alpha_{8,9} - \alpha_{9,10})$ | $\delta$ NCN' |
| 20. | $S_{20} = \frac{1}{\sqrt{6}}(2\alpha_{3,4} - \alpha_{3,5} - \alpha_{4,5})$ | $\delta_a$ $CH_3$ |
| 21. | $S_{21} = \frac{1}{\sqrt{6}}(2\alpha_{2,5} + \alpha_{2,3} + \alpha_{2,4} - \alpha_{3,4} - \alpha_{3,5} - \alpha_{4,5})$ | $\delta_s$ $CH_3$ |
| 22. | $S_{22} = \frac{1}{\sqrt{6}}(2\alpha_{2,5} - \alpha_{3,5} - \alpha_{4,5})$ | $\rho$ $CH_3$ |
| 23. | $S_{23} = \frac{1}{\sqrt{2}}(d_4 - d_3)$ | $\nu_a$ $CH_3$ |

| | | |
|---|---|---|
| 24. | $S_{24} = \frac{1}{\sqrt{2}}(\alpha_{4,5} - \alpha_{3,5})$ | $\delta$ $CH_3$ |
| 25. | $S_{25} = \frac{1}{\sqrt{2}}(\alpha_{2,3} - \alpha_{2,5})$ | $\rho$ $CH_3$ |
| 26. | $S_{26} = \frac{1}{\sqrt{2}}(\tau_{4325} + \tau_{9325} - \tau_{4321} - \tau_{9321})$ | $\pi$ $C^{'}O$ |
| 27. | $S_{27} = \frac{1}{\sqrt{8}}(\tau_{1091112} + \tau_{1091113} - \tau_{10934} - \tau_{10932} + \tau_{43911} + \tau_{23911} - \tau_{391112} - \tau_{391113})$ | $\pi$ CS |
| 28. | $S_{28} = \frac{1}{\sqrt{8}}(\tau_{43910} + \tau_{43911} + \tau_{1239} + \tau_{5239} - \tau_{5234} - \tau_{1234} - \tau_{23910} - \tau_{23911})$ | $\pi$ $N^{'}H$ |
| 29. | $S_{29} = \frac{1}{\sqrt{6}}(\tau_{5216} + \tau_{5217} + \tau_{5218} + \tau_{3216} + \tau_{3217} + \tau_{3218})$ | $\tau$ $CH_3$ |
| 30. | $S_{30} = \frac{1}{\sqrt{2}}(\tau_{5234} + \tau_{1234} + \tau_{5239} + \tau_{1239})$ | $\tau$ $C^{'}N^{'}$ |
| 31. | $S_{31} = \frac{1}{\sqrt{2}}(\tau_{23910} + \tau_{23911} + \tau_{43910} + \tau_{43911})$ | $\tau$ $CN^{'}$ |
| 32. | $S_{32} = \frac{1}{\sqrt{2}}(\tau_{1091113} + \tau_{1091112} + \tau_{391113} + \tau_{391112})$ | $\tau$ $NH_2$ |
| 33. | $S_{33} = \frac{1}{\sqrt{2}}(\tau_{1091113} - \tau_{1091112} + \tau_{391113} + \tau_{391112})$ | $\omega$ $NH_2$ |

**Table 3. Experimental and B3LYP levels computed Vibrational ($cm^{-1}$) obtained for NATU**

| Model No | Experimental frequency $cm^{-1}$ | | Observed frequency $Cm^{-1}$ | | Assignments |
|---|---|---|---|---|---|
| | FT-IR | FT-RAMAN | 6-311G(d,p) | 6-311G++(d,p) | |
| 1. | 3793 | - | 3735 | 3732 | $\nu_{as}NH_2$(100) |
| 2. | 3383 | 3287 | 3221 | 3218 | $\nu_{s}NH_2$(100) |
| 3. | 3275 | 3237 | 3190 | 3185 | $\nu_{s}$NH(99) |
| 4. | 3177 | 3183 | 3155 | 3152 | $\nu_{a}CH_3$(100) |
| 5. | 2785 | - | 2763 | 2762 | $\nu_{s}CH_3$(100) |
| 6. | 2685 | - | 2705 | 2705 | $\nu$ C0(69), $\nu$ CN(15) |
| 7. | 1817 | - | 1788 | 1766 | $\delta$ $NX_2$(76), $\nu$ CN(20) |
| 8. | 1614 | 1613 | 1642 | 1639 | $\nu$ CN'(36), $\delta$ NX(31) |
| 9. | 1519 | - | 1514 | 1512 | $\delta_{a}CH_3$(58), $\delta$ CN(17) |
| 10. | 1472 | 1465 | 1495 | 1493 | $\nu$ CN(40), $\delta_{a}CH_3$(22) |
| 11. | 1446 | - | 1439 | 1439 | $\delta_{s}CH_3$(83) |
| 12. | 1411 | 1384 | 1437 | 1384 | $\delta$ NX(35). $\nu$ CC(16), $\nu$ CN(15) |
| 13. | 1396 | - | 1389 | 1391 | $\delta$ $NX_2$(33), $\nu$ CS(17), $\delta$ NCN(16) |
| 14. | 1286 | - | 1296 | 1246 | $\nu$ $CH_3$(31), $\nu$ CC(28), $\nu$ $NX_2$(19) |
| 15. | 1223 | - | 1255 | 1254 | $\nu$ $CH_3$(64) |
| 16. | 1083 | 1094 | 1062 | 1058 | $\nu$ CN'(32), $\rho$ $NX_2$(26), $\nu$ C'S(18) |
| 17. | 1045 | 1050 | 1056 | 1051 | $\nu$ CS(40), $\nu$ $NX_2$(40) |
| 18. | 1008 | 1010 | 1011 | 1012 | $\delta$ CO(48), $\nu$ CS(19) |
| 19. | 868 | | 854 | 856 | $\delta$ CS(43), $\delta$ CO(19), $\delta$ NCN(19) |
| 20. | 813 | | 802 | 802 | $\delta$ NCN(36), $\delta$ CCN(29), $\delta$ CS(19) |
| 21. | 729 | 734 | 738 | 725 | $\delta$ CCN(39), $\delta$ CS(19) |
| 22. | 630 | | 624 | 615 | $\delta$ CNC(65) |
| 23. | 570 | 570 | 567 | 560 | $\nu$ $CH_3$(100) |
| 24. | 563 | | 559 | 559 | $\delta$ $CH_3$(93) |

| | | | | | |
|---|---|---|---|---|---|
| 25. | 539 | | 533 | 532 | $\rho$ $CH_3$(86) |
| 26. | 503 | 479 | 509 | 496 | $\tau$ $NX_2$(99) |
| 27. | 396 | | 380 | 368 | $\varpi$ $NX_2$(73) |
| 28. | 319 | | 316 | 305 | $\tau$ CN'(43), $\varpi$ $NX_2$(26) |
| 29. | 296 | 298 | 302 | 291 | $\pi$ CO(87) |
| 30. | 224 | 218 | 222 | 215 | $\pi$ CS(68), $\pi$ NH(21) |
| 31. | - | 116 | 126 | 117 | $\tau$ $CH_3$(95) |
| 32. | - | 65 | 78 | 75 | $\tau$ CN'(43), $\tau$ CN(34) |
| 33. | 62 | | 68 | 65 | $\pi$ N'X(55), $\tau$ CN'(24) |

**Table 4. Comparative values of IR intensity and Raman activity between B3 LYP/6-311++G (d, p) of NATU**

| S.NO | ASSINGMENT | IR INTENSITY | RAMAN INTENSITY | REDUCED MASS | FORCE CONSTANT | POLARISED | UNPOLARISED |
|---|---|---|---|---|---|---|---|
| 1 | $\nu_a$ $NH_2$ | 13.5 | 45.9 | 1.1052 | 9.0863 | 0.6562 | 0.7924 |
| 2 | $\nu_s$ $NH_2$ | 8.3 | 100.0 | 1.0448 | 8.0262 | 0.1438 | 0.2514 |
| 3 | $\nu$ NH | 9.1 | 30.6 | 1.076 | 8.1096 | 0.1395 | 0.2449 |
| 4 | $\nu$ CN | 0.5 | 73.3 | 1.098 | 6.4393 | 0.5164 | 0.6811 |
| 5 | $\nu$ CN' | 0.9 | 29.9 | 1.1019 | 6.2294 | 0.75 | 0.8571 |
| 6 | $\nu$ C'N' | 0.9 | 88.8 | 1.0391 | 5.6279 | 0.0105 | 0.0207 |
| 7 | $\nu$ CS | 54.6 | 31.6 | 8.2676 | 15.5747 | 0.2564 | 0.4082 |
| 8 | $\nu$ C'O | 30.7 | 2.4 | 1.3018 | 2.0683 | 0.7495 | 0.8568 |
| 9 | $\nu$ CC' | 34.6 | 5.7 | 1.5665 | 2.1143 | 0.3427 | 0.5105 |
| 10 | $\nu_s$ $CH_3$ | 1.9 | 8.5 | 1.0458 | 1.3773 | 0.75 | 0.8571 |
| 11 | $\nu_a$ $CH_3$ | 14.8 | 5.4 | 1.1305 | 1.4784 | 0.5904 | 0.7425 |
| 12 | $\delta$ NH | 20.6 | 15.7 | 3.7754 | 4.5947 | 0.2511 | 0.4015 |
| 13 | $\rho$ $NH_2$ | 13.9 | 0.8 | 1.3629 | 1.5495 | 0.7404 | 0.8508 |
| 14 | $\delta$ CS | 100.0 | 6.0 | 2.6736 | 2.6555 | 0.7288 | 0.8431 |
| 15 | $\delta$ NH | 4.7 | 0.8 | 2.4378 | 2.2631 | 0.6199 | 0.7654 |
| 16 | $\delta$ CNC | 7.1 | 1.5 | 2.3255 | 1.5448 | 0.5501 | 0.7098 |
| 17 | $\delta$ CO | 0.9 | 0.1 | 1.7459 | 1.1474 | 0.75 | 0.8571 |
| 18 | $\delta$ CCN | 7.1 | 1.6 | 1.6663 | 1.0044 | 0.2994 | 0.4608 |
| 19 | $\delta$ NCN' | 5.5 | 5.1 | 3.1306 | 1.3445 | 0.1834 | 0.31 |
| 20 | $\delta_a$ $CH_3$ | 0.3 | 13.9 | 4.3148 | 1.6363 | 0.123 | 0.219 |
| 21 | $\delta_s$ $CH_3$ | 14.2 | 0.9 | 1.1583 | 0.403 | 0.75 | 0.8571 |
| 22 | $\rho$ $CH_3$ | 0.1 | 3.4 | 9.0954 | 2.0843 | 0.75 | 0.8571 |
| 23 | $\nu_a$ $CH_3$ | 0.8 | 0.4 | 1.8599 | 0.352 | 0.75 | 0.8571 |
| 24 | $\delta$ $CH_3$ | 5.4 | 2.5 | 3.4679 | 0.6393 | 0.254 | 0.4051 |
| 25 | $\rho$ $CH_3$ | 1.2 | 3.6 | 5.6182 | 0.9397 | 0.2696 | 0.4247 |
| 26 | $\pi$ C'O | 2.0 | 2.2 | 1.2178 | 0.2021 | 0.75 | 0.8571 |
| 27 | $\pi$ CS | 0.4 | 2.1 | 3.9812 | 0.3396 | 0.479 | 0.6477 |
| 28 | $\pi$ N'H | 1.2 | 3.6 | 4.3902 | 0.2582 | 0.444 | 0.6149 |
| 29 | $\tau$ $CH_3$ | 5.1 | 0.2 | 1.0262 | 0.0550 | 0.75 | 0.8571 |
| 30 | $\tau$ C'N' | 1.3 | 1.3 | 6.5178 | 0.1900 | 0.606 | 0.7547 |
| 31 | $\tau$ CN' | 4.0 | 0.5 | 3.0263 | 0.0283 | 0.75 | 0.8571 |
| 32 | $\tau$ $NH_2$ | 3.3 | 0.3 | 5.7438 | 0.0206 | 0.75 | 0.8571 |
| 33 | $\omega$ $NH_2$ | 12.9 | 1.0 | 1.3636 | 0.0098 | 0.75 | 0.8571 |

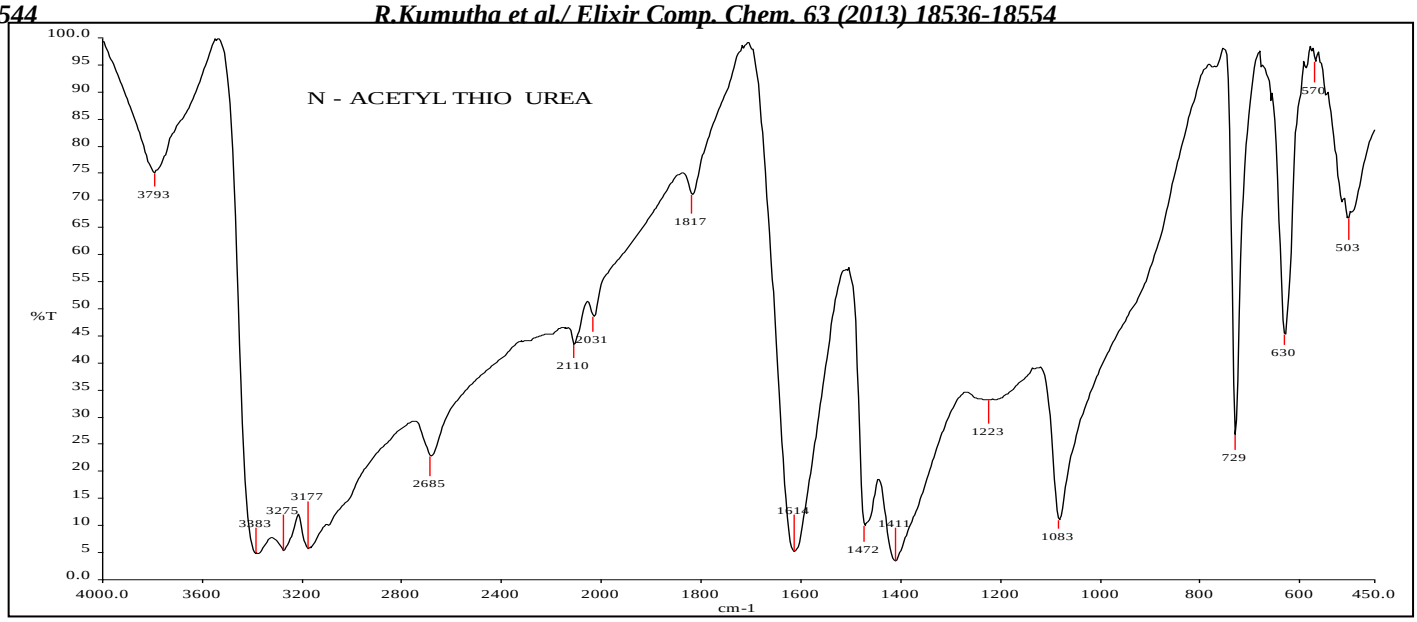


**Fig 2. Experimental Observed FT-IR Spectrum of N-Acetyl Thiourea**

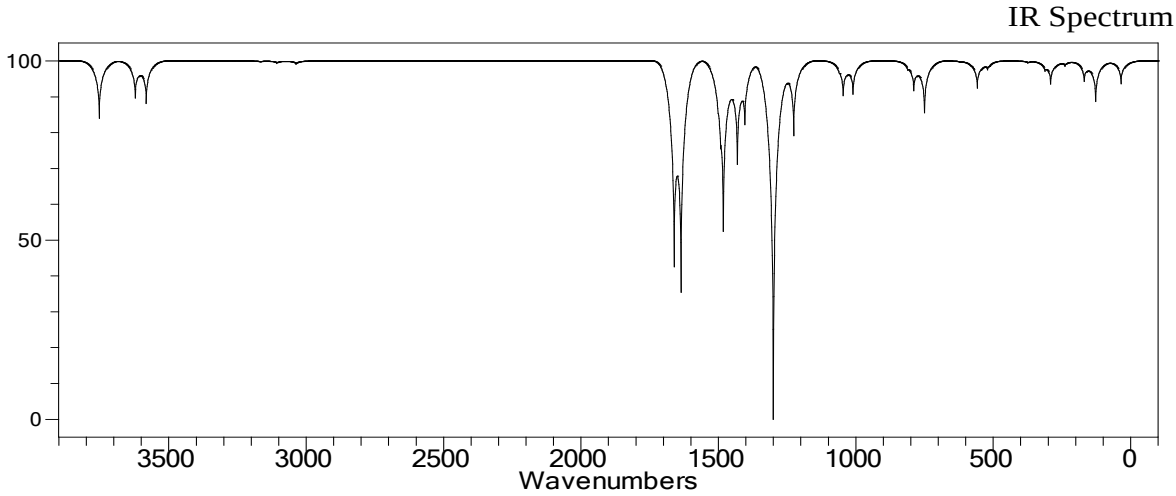


**Fig 2a. Theoretical IR Spectrum of N-acetylthiourea**

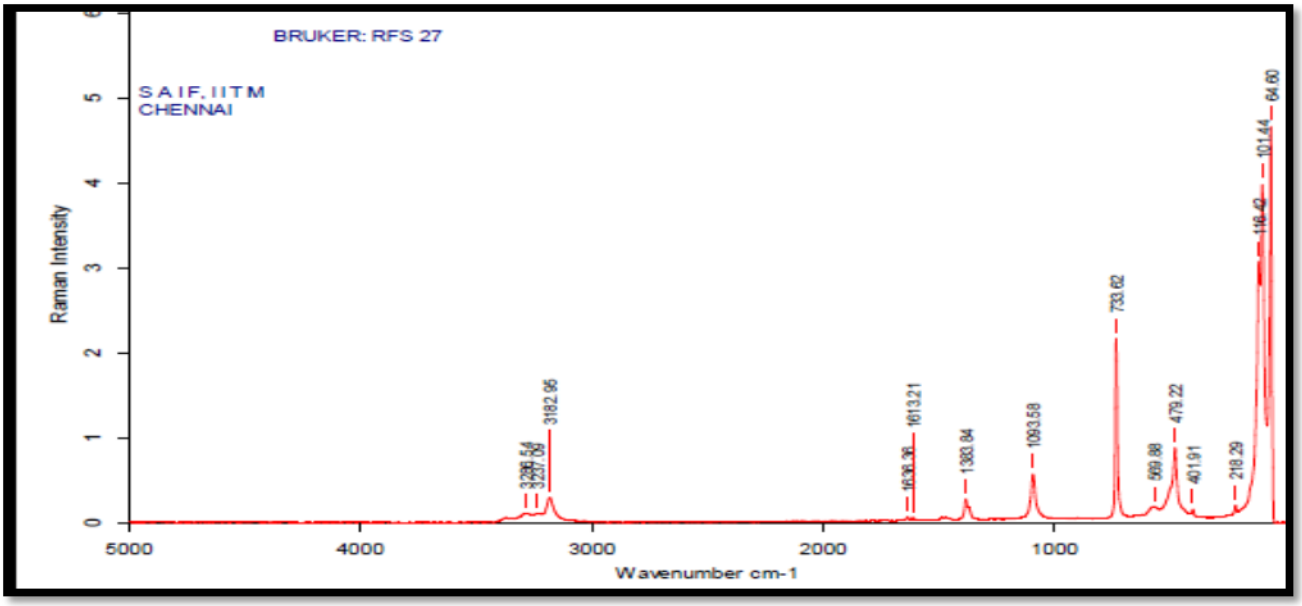


**Fig 3a. Experimental Observed FT-Raman Spectrum of N-Acetyl Thiourea**

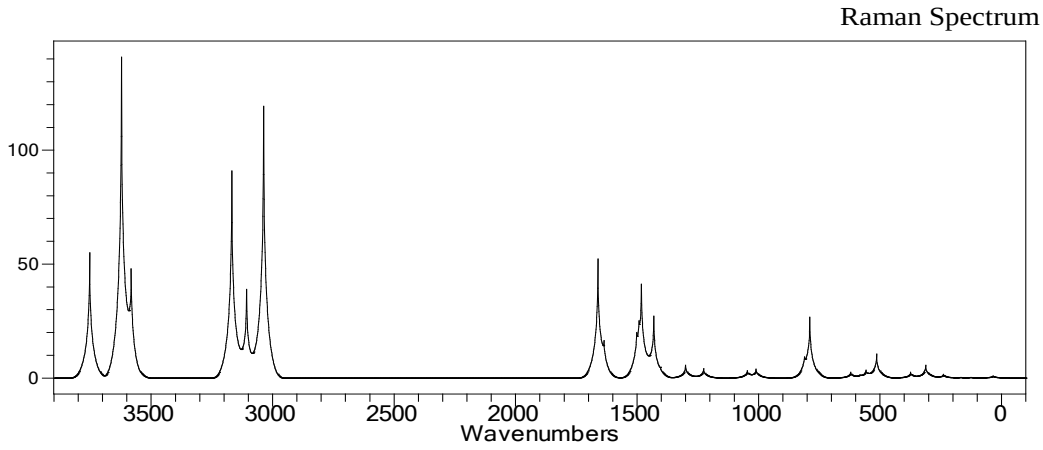


**Fig 3b. Theoretical Raman Spectrum of N-acetylthiourea**

The Infrared and Raman spectra of NATU are shown in Figures 2, 2a, 3 and 3a. The observed frequencies are compared with calculated frequency for NATU. The calculated potential energy distributions are also shown along with the assignment in Table 3. The calculated $NH_2$ asymmetric stretching vibrations give rise to the strong band at 3732 cm-$^{1}$ compare with the experimental result at 3793 cm-$^{1}$. The theoretical observed $NH_2$ symmetric stretching vibration give rise to the strong band at 3218 cm$^{-1}$ compare with the experimental value at 3287 cm$^{-1}$. The band at 2705 cm-$^{1}$ in NATU is due to the CO stretching vibrations well agree with the experimental results. The band at 1010 cm-$^{1}$ in NATU is assigned to the CO in plane bending vibration. According to the potential energy distribution the CO in plane bending mode contribute 19% to the 856 cm-$^{1}$ band observed for the CS in plane deformation. The other characteristics band of interest are due to the C=S and C-N stretching vibration and NH in plane bending corresponding to the thioamide 1,2 ,and 3 bands respectively. The result indicate a delocalized CS mode contributing cheaply to the 1045 cm-$^{1}$ band akin to the 1020 cm-$^{1}$ band thiosemicarbozide [32,33] and in contrast to a localized C=S stretching mode of N—methyl thioureaat 998 cm-$^{1}$. The CS frequency of NATU is higher than that in thiourea and symmetric N,N'-dimethylthiourea assigned in a 980 cm-$^{1}$. In Monothiopiuret which is isoelectronic with NATU, the CS stretching is assigned at 1015 cm-$^{1}$.

The high and low C-N stretching frequency (amide III band) corresponding to asymmetric and symmetric are studies under Density Functional Theory (DFT) are close agree with experimental values. The thioamide II band of CS,$NH_2$ group due to NH bonding is observed 3185 cm-$^{1}$ is quite agree with the theoretical values.

The thioamide II band of the -$CSHN_2$- group due to $NH_2$ bending is observed at 1817 cm$^{-1}$ which is higher than the 1642 cm$^{-1}$ band of NMTU. The thioamide II of –CSNH- grouping contributes to two bands at 1614 and 1384 cm$^{-1}$. The analogous NH bending frequencies are found in the region 1350 to 1400 cm$^{-1}$ in NMTU [34], DMTU[35,36] and thio-semicarbazide [32,33] . The thioamide VI band due to the in plane C=S bending occurs at 868 cm$^{-1}$ as in the case of thioacetamide [37,38]. In contrast, NMTU exhibits a more delocalized C=S bending mode. The assignments of other frequencies are compatible with the general features of NMTU sym. DMTU and monothioiuret [39] The very low frequency bands assigned for the out of plane modes corresponding to the torsion at 116 cm$^{-1}$, the NH out –of-plane ending mode at 62 cm$^{-1}$ and the band at 65 cm$^{-1}$ due to CN torsion Moreover, these modes may expected to mix strongly with the centre of mass motions, due to their proximity to the lattice modes.

**Natural bond orbital (NBO) analysis**

The $E^{(2)}$ value is chemically significant and can be used as a measure of the intra molecular delocalization. These results are presented in Table 5. The Natural bond orbital analysis provides an efficient method for studying intra and intermolecular bonding and interaction among bonds, and also provides a convenient basis for investigating charge transfer or conjugative interaction in molecular systems. Some electron donor orbital, acceptor orbital and the interacting stabilization energy resulting from the second-order micro disturbance theory are reported [40,41]. The result of interaction is a loss of occupancy from the concentration of electron NBO of the idealized Lewis structure into an empty non-Lewis orbital. For each donor ($i$) and acceptor ( $j$), the stabilization energy $E(2)$ associated with the delocalization $i \rightarrow j$ is estimated as

$$E(2) = -n_\sigma \frac{\langle \sigma | F | \sigma \rangle^2}{\varepsilon_\sigma^2 - \varepsilon_\sigma} = -n_\sigma \frac{F_{ij}^{\ 2}}{\Delta E}$$

Where $\langle \sigma | F | \sigma \rangle^2$ or $F_{ij}^{\ 2}$ is the Fock matrix element *i* and *j* NBO orbitals, $\varepsilon_\sigma^*$ and $\varepsilon_\sigma$ are the energy of the $\sigma$ and $\sigma$* NBOs and $n_\sigma$ is the population of the donor $\sigma$ orbital.

**Table 5. Second order perturbation theory analysis of Fock matrix in NBO basis**

| Donor(i) | Type | ED(e) | Acceptor(j) | Type | ED(e) | E(2) [a] (kJ/mol) | E(j)–E(i) [b] (a.u.) | F(i, j) [c] (a.u.) |
|---|---|---|---|---|---|---|---|---|
| N1-C2 | σ | 1.98760 | N1-C5 | σ* | 0.08003 | 1.66 | 1.30 | 0.042 |
| N1-C2 | σ | 1.98760 | NI-H8 | σ* | 0.01532 | 0.70 | 1.26 | 0.027 |
| N1-C2 | σ | 1.98760 | C2-S3 | π* | 0.01169 | 1.02 | 1.25 | 0.032 |
| N1-C2 | σ | 1.98760 | N4-H9 | σ* | 0.00940 | 1.69 | 1.28 | 0.041 |
| N1-C5 | σ | 1.98790 | N1-C2 | σ* | 0.06521 | 2.81 | 1.28 | 0.048 |
| N1-C5 | σ | 1.98790 | C5-O6 | σ* | 0.01210 | 1.05 | 1.46 | 0.035 |
| N1-H8 | σ | 1.98168 | C2-N4 | σ* | 0.05483 | 4.54 | 1.12 | 0.064 |
| N1-H8 | σ | 1.98168 | C5-C7 | σ* | 0.05844 | 3.50 | 1.04 | 0.054 |
| C2-S3 | π | 1.98088 | N1-C5 | σ* | 0.08003 | 3.67 | 1.22 | 0.061 |
| C2-N4 | σ | 1.99150 | N1-C2 | σ* | 0.06521 | 0.79 | 1.28 | 0.029 |
| C2-N4 | σ | 1.99150 | N1-H8 | σ* | 0.01532 | 1.89 | 1.25 | 0.044 |
| C2-N4 | σ | 1.99150 | C2-S3 | π* | 0.01169 | 1.19 | 1.24 | 0.034 |
| N4-H9 | σ | 1.98741 | N1-C2 | σ* | 0.06521 | 5.46 | 1.10 | 0.070 |
| N4-H10 | σ | 1.98005 | C2-S3 | π* | 0.01169 | 3.83 | 1.08 | 0.058 |
| C5-O6 | σ | 1.99297 | N1-C5 | σ* | 0.08003 | 1.10 | 1.52 | 0.037 |
| C5-O6 | π | 1.98348 | C7-H12 | σ* | 0.01126 | 1.85 | 0.71 | 0.032 |
| C5-C7 | σ | 1.98726 | N1-H8 | σ* | 0.01532 | 2.61 | 1.08 | 0.047 |
| C7-H11 | σ | 1.98326 | C5-O6 | σ* | 0.01210 | 1.20 | 1.14 | 0.033 |
| C7-H12 | σ | 1.94332 | N4-H10 | σ* | 0.08096 | 20.96 | 0.98 | 0.129 |
| C7-H12 | σ | 1.94332 | C5-O6 | π* | 0.23607 | 4.59 | 0.55 | 0.047 |
| C7-H13 | σ | 1.94327 | C5-O6 | σ* | 0.01210 | 1.34 | 1.16 | 0.036 |
| S3 | LP2 | 1.88202 | N1-C2 | σ* | 0.06521 | 14.92 | 0.62 | 0.087 |
| S3 | LP2 | 1.88202 | C2-N4 | σ* | 0.05483 | 14.26 | 0.63 | 0.086 |
| N4 | LP1 | 1.72300 | C2-S3 | σ* | 0.42941 | 65.72 | 0.22 | 0.111 |
| N4 | LP1 | 1.72300 | C7-H13 | σ* | 0.01127 | 1.04 | 0.59 | 0.024 |
| O6 | LP2 | 1.97781 | C5-C7 | σ* | 0.05844 | 2.09 | 1.04 | 0.042 |
| O6 | LP2 | 1.87116 | N1-C5 | σ* | 0.08003 | 25.20 | 0.70 | 0.120 |
| O6 | LP2 | 1.87116 | C5-C7 | σ* | 0.05844 | 20.40 | 0.62 | 0.102 |

[a] E (2) means energy of hyper conjugative interaction (stabilization energy).

[b] Energy difference between donor and acceptor i and j NBO orbitals.

[c] F(i,j) is the Fock matrix element between i and j NBO orbitals.

The intra molecular interaction is formed by the orbital overlap between σ(C-N) and σ*(C-N) which results into intra-molecular charge transfer using stabilization of the system. The electron density of $N_4$-$H_9$ is 1.98741 ev. The most important interactions in the title compound having lone pair $O_6$ with that of antibonding $N_1$-$C_5$ and $C_s$-$C_7$ results into the stabilization of 25.20 and 20.40 KJ/mol, respectively. The interactions between lone pair $N_4$ with anti-bonding $C_2$-$S_3$,and $C_7$-$H_{13}$ results into the stabilization of 65.72 and 1.04 KJ/mol, respectively, which denotes larger delocalization. The interaction between the lone-pair LP2 and the anti-bonding orbital σ*($C_5$-$C_7$) is 2.09 KJ/Mol, which is weaker than those of LP2 and σ*($N_1$-$C_5$), LP2 and σ*($C_5$-$C_7$) but bigger than those of LP1 and σ*($C_7$-$H_{13}$).

**Hyper polarizability**

The first hyperpolarizability (β) of this novel molecular system and relates properties (β,α,and Δα) of ATU which calculated using B3LYP/6.311++G(d,p) basis set, based on the finite-field approach and are presented in Table 6. In the presence of an applied electric field, the energy of system is the function of the electric field. Polarizability and hyperpolarizability characterize the response of a system in an applied electric field [42] They determine not only the strength of molecular interactions and the cross sections of different scattering and collision process but also the non-linear optical properties (NLO) of the system [43,44]. First hyperpolarizability is a third-rank tensor that can be described by 3*3*3 matrix. The 27 component of the 3D matrix can be reduced to 10 components due to the Kleiman symmetry [45]. It can be given in the lower tetrahedral format. It is obvious that the lower part

of the 3*3*3 matrices is a tetrahedral components of β are defined as coefficients in the Taylor series expansion of the energy in the external electric field. When the external electric field is weak and homogeneous, this expansion becomes as follows.

$E= E^{o} -\mu_i F_i/1! - \alpha_{ij}F_iF_J/2! - \beta_{ijk}F_iF_JF_K/3! - \nu_{ijkl}F_iF_jF_KF_l/4! +\ldots\ldots$

Where $E_o$ is the energy of the unperturbed molecules, $F_\alpha$ is the field at the origin, and $\mu_\alpha$, $\alpha_{\alpha\beta}$, $\beta_{\alpha\beta\nu}$ are the component of dipole moment, polarizability and the first hyper polarizability respectively.

The total static dipole moment is $\mu = (\mu^2_x +\mu^2_y+\mu^2_z)^{1/2}$

T he isotropic polarizability is $\alpha = \alpha_{xx}+\alpha_{yy}+\alpha_{zz}/3$

The polarizability anisotropy invariant is $\Delta\alpha = 2^{-1/2} [(\alpha_{xx}-\alpha_{yy} )+ (\alpha_{yy}-\alpha_{zz})][(\alpha_{zz}-\alpha_{xx})^2+6\alpha^2_{xz}]^{1/2}$

$$\beta_{tot} = (\beta^2_x+\beta^2_y+\beta^2_z)^{1/2}$$

$$\beta_x = \beta_{xxx}+ \beta_{xyy} +\beta_{xzz}$$

$$\beta_y =\beta_{yyy}+\beta_{xxy}+\beta_{yzz}$$

$$\beta_z =\beta_{zzz}+\beta_{xxz}+\beta_{yyz}$$

And the average hyper polarizability is $\beta_{tot} = (\beta^2_x+\beta^2_y+\beta^2_z)^{1/2}$

**Table 6. B3LYP/6-311++G(d,p) calculated electric dipole moments (Debye), polarizability (in a A.U.), β components and βtot ($10^{-31}$ esu) value of NATU**

| Parameter | B3LYP/6-311++(d, p) | Parameter | B3LYP/6-311++(d, p) |
|---|---|---|---|
| μx | 1.1661 | $\beta_{xxx}$ | 90.7509 |
| μy | -1.2123 | $\beta_{xxy}$ | 99.1943 |
| μz | 0.0001 | $\beta_{xyy}$ | 10.3502 |
| μ | 1.6821 | $\beta_{yyy}$ | -222.6454 |
| $\alpha_{xx}$ | 66.5622 | $\beta_{xxz}$ | -0.6039 |
| $\alpha_{xy}$ | 6.9891 | $\beta_{xyz}$ | 0.1839 |
| $\alpha_{yy}$ | 104.0211 | $\beta_{yyz}$ | 0.3926 |
| $\alpha_{xz}$ | -0.0002 | $\beta_{xzz}$ | 29.3536 |
| $\alpha_{yz}$ | -0.0008 | $\beta_{yzz}$ | -25.1185 |
| $\alpha_{zz}$ | 35.8571 | $\beta_{zzz}$ | -0.24953 |
| α | 68.8134 | $\beta_{tot}$ (esu) | $1.7081 \times 10^{-30}$ |
| Δα | $1.9202 \times 10^{-23}$ | | |

Where E is the energy of the unperturbed molecules, $F_i$ is the Field at the origin and $\mu_i$, $\alpha_{ij}$, $\beta_{ijk}$ and $\nu_{ijkl}$ are the components of dipole moment, polarizability, first hyperpolarizability and the second hyperpolarizability, respectively. The total static dipole moment μ, the mean polarizability α, the anisotropy of the polarizability (Δα) and the first hyperpolarizability $\beta_{tot}$ using the x, y, z component, are defined. The B3LYP/ 6.311++G(d,p) calculated the first hyperpolarizability of NATU is $1.7081 \times 10^{-30}$esu. Which is five times greater than the value of urea is ( $0.372 \times 10^{-30}$esu ). The total molecular dipole moment (μ), mean polarizability α and anisotropy polarizability (Δα) of NATU have been calculated the hyperpolarizability of other molecules reported earlier [46,47] the value of first hyperpolarizability of NATU molecule possesses non-linear optical properties that can be used for NLO applications.

**Mulliken atomic charges**

The Mulliken procedure is the most common population analysis technique. In population analysis, the electrons in each molecular orbital are partitioned to each atom based on the probability that the electron is in an orbital on that atom at the end of the calculation the fractional occupation for each molecular orbital is summed to get a total atomic electron population for each atom[48]. Mulliken charges arising from the Mulliken population analysis provides a mean of estimating partial atomic charges from calculations carried out by the methods of computational chemistry, particularly those based on the linear combination of atomic orbitals molecular orbital method.

Mulliken atomic charge calculation has an important role in the application of quantum chemical calculation to molecular system because of atomic charges effect dipole moment, molecular polarizability, electronic structure and a lot of properties of molecular systems. The charge distributions over the atoms suggest the formation of donor and acceptor pairs involving the charge transfer in the

molecule. The Mulliken population analysis in NATU molecule is calculated using B3LYP level with 6-311++G(d,p) basis set are listed in Table 7. From the result, it is clear that the substitution $NH_2$ atoms in the aromatic ring lead to a redistribution of electron density. The σ electron with drawing character of the atom in NATU is demonstrated by the decrease of electron density on $C_7$ and $S_3$ atoms. The atomic charges in the $NH_2$ groups are almost identical. The Mulliken charge obtained from 6.311++G(d,p) basis set shown in Table 7 that $H_8$ and $H_9$ atoms are more acidic due to more +ve charge.

**Table 7. Mullikan atomic charges calculated by B3LYP/6-311++G(d,p) method**

| Atom No | B3LYP/ 6-311++G(d,p) | Atom No | B3LYP/ 6-311++G(d,p) |
|---|---|---|---|
| N1 | -0.0836 | H8 | 0.3156 |
| C2 | 0.0870 | H9 | 0.2949 |
| S3 | -0.5103 | H10 | 0.2852 |
| N4 | -0.3365 | H11 | 0.2139 |
| C5 | 0.2170 | H12 | 0.1715 |
| O6 | -0.2890 | H13 | -0.0836 |
| C7 | -0.5371 | | |

The Mulliken charge analysis of NATU shows that presence of Oxygen and Sulfur ( $O_6$ = -0.2890,$S_3$=-0.5103 imposes positive charges on $C_5$, and $C_2$ atoms. However,$H_8$, $H_9$, $H_{10}$ possess positive charge due to large negative charge nitrogen atoms($N_1$=-0,0836 and $N_4$=-0,3365).

**Frontier molecular orbital analysis**

The conjugated molecules are characterized by the separation between highest occupied molecular orbital and lowest unoccupied molecular orbital (HOMO-LUMO), which is the result of a Significant degree of intramolecular charge transfer (ICT) from the end-capping electron-donor groups through π-conjugated path. The strong charge transfer interaction through π-conjugated bridge results in substantial ground state donor-acceptor mixing and the appearance of a charge transfer band in the electronic absorption spectrum. Therefore, an ED transfer occurs from the more aromatic part of the π-conjugated system in the electron-donor side to its electron withdrawing part the aromatic orbital components of the frontier molecular orbitals are shown in Figs (4a to 4f). From the figure Properties of N-acetyl thioureathe molecular orbitals from HOMO-2 to LUMO+2 of NATU, in which all the LUMO surfaces are well localized. In other words all intermolecular interactions are mostly occurred in LUMO levels. In HOMO-1, $S_1$ is highly coupled with $H_9$, $N_1$, and $O_6$. Moreover, $C_1$ and $S_1$ interaction is also present in this orbital. Most of the surfaces shown in the HOMO side have no amplitude on $CH_3$ group.

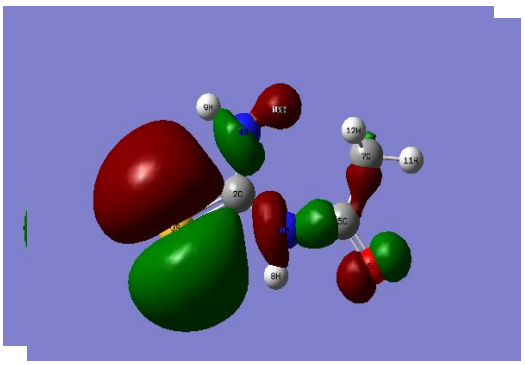

**(a)HOMO**

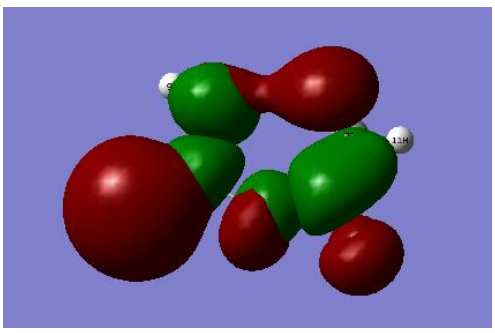

**(b) LUMO**

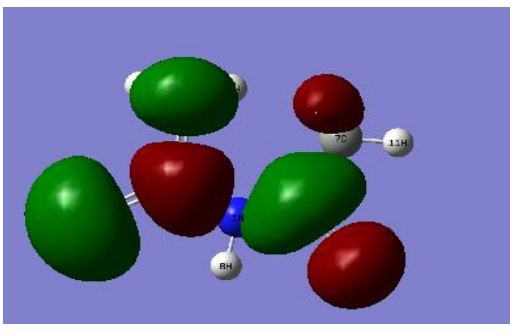

**(c) HOMO-1**

**(d) LUMO+1**

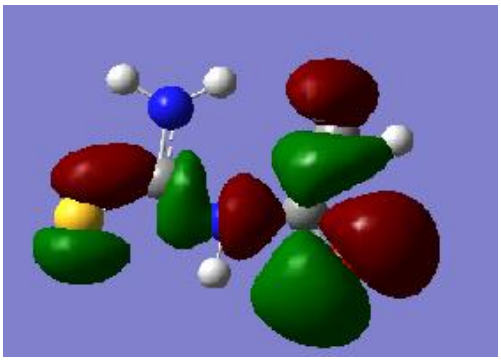

(e) HOMO-2

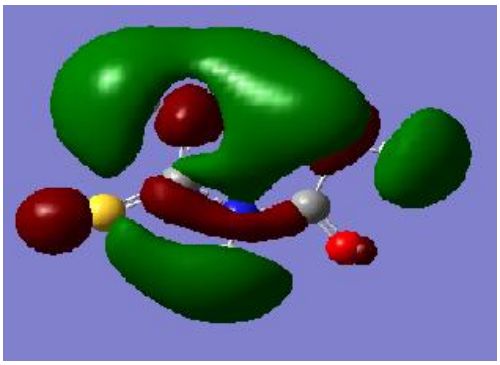

(f) LUMO-2

**Fig 4. HOMO- LOMO Picture of NATU**

The presence of intramolecular charge transfer from donor to acceptor group within molecule can be identified by analyzing the co-existence of IR and Raman activity itself. It is also observed that in our NATU that the bands at 3383, 1614, 1045, and 570 $cm^{-1}$ in FT-IR spectrum have their counterparts in FT-Raman at 3287,1613,1050 and 570 $cm^{-1}$, which shows that the relative intensities in IR and Raman are comparable resulting from the electron cloud movement through single-double bond π-conjugated path from donor to acceptor groups. The analysis of wave function indicates that the electron absorption corresponds to the transitions from the ground state to the first exited state and is mainly described by one –electron excitation from the HOMO to LUMO. The HOMO and LUMO energies of NATU have been calculated at B3LYP/6.31G (d,p) level which is presented in Table 8. The energy gap presented in Table 8 reflects the chemical activity of the molecule. HOMO represents the ability to donate an electron and LUMO represents the ability to accept an electron. Among four the subsequent excited states calculated, the strongest transitions appear between HOMO-LUMO orbitals. The numerical value of energy gap between HOMO-LUMO orbitals calculated at B3LYP level. The energy gaps for other possible energy transitions are presented in Table 8.

**Table 8. Selected HOMO and LUMO energies of NATU.**

| S.NO | MOLECULAR ORBITAL | ENERGY eV | MOLECULAR ORBITAL ENERGY TRANSITIONS | ENERGY GAP eV |
|---|---|---|---|---|
| 1. | HOMO | -8.812 | HOMO→LUMO | -9.612 |
| 2. | HOMO-1 | 0.8000 | HOMO-1→LUMO | -11.741 |
| 3. | HOMO-2 | -10.941 | HOMO-2→LUMO | -12.832 |
| 4. | LUMO | 9.113 | HOMO→LUMO+1 | -17.925 |
| 5. | LUMO+1 | -12.032 | HOMO-1→LUMO+1 | -20.054 |
| 6. | LUMO+2 | 41.235 | HOMO-2→LUMO+1 | -21.145 |
| 7. | | | HOMO→LUMO+2 | -50.047 |
| 8. | | | HOMO-1→LUMO+2 | -52.176 |
| 9. | | | HOMO-2→LUMO+2 | -53.267 |

**Fukui function**

DFT is one of the important tools of quantum chemistry to understand popular chemical concepts such as electronegativity, electron affinity, chemical potential and ionisation potential. In order to solve the negative Fukui function problem, different attempts have been made by various groups Kolandaivel et al [49] introduced the atomic descriptor to determine the local reactive sites of the molecular system. This is important in the use of the Fukui function of an intramolecular reactivity index. From the results of Tables 7& 8, the $(\delta f_a)_k$ were calculated and reported in Table 9. From Table 9, note the presence of negative fukui function value means that when adding on e to the molecule, in some spots, the electron density reduced, alternatively when removing an electron from the molecule in some spots, the electron density is increased has related this behavior with reduction and oxidation of atomic centers into the molecule. From the values reported in Table 9, the reactivity order for the electrophilic attack was found exclusively on the $0_6$>$N_4$>N1 thiocarbonyl ring.. This may be due to steric effects the reactivity in the ring might be difficult. On the other hand, for nucleophilic attack, the reactivity order was $N_1$>$H_8$>$H_9$ Note that the positions of reactive nucleophilic sites are mainly located on the pyrrole ring. It was observed a less reactivity for this kind of attack in comparison with the electrophilic attack $(sf^{+/-})_p$ redacts the

most nucleophilic and electrophilic in a molecule is the one which has the maximum $(sf^{+/-})_k$ value, which in turn is the softest region in a molecule.

**Molecular electrostatic potential surface**

MEP has been used primarily for predicting sites and relative reactivates towards electrophilic and nucleophilic attack, and is studies of biological recognition and hydrogen bonding interactions [50, 52] . The calculated 3D MEP of the title compound was calculated from optimized molecular structure by using B3LYP/6.311++G level and also shown in Figure 5. According to the results, the negative region (red) is mainly over the N,C, and H atomic sites, which were caused by the contribution of lone –pair electrons of nitrogen and Carbon atom while the positive (blue) potential sites are around the oxygen & sulphur atoms. A portion of a molecule that has a negative electrostatic potential will be susceptible to electrophilic attack the more negative is the better. It is not as straight forward to use electrostatic potentials to predict nucleophilic attack. Hence the negative region (red) and positive region (blue) indicate electrophilic and nucleophilic attack symptoms. Also a negative electrostatic potential region is observed around the $O_6$ atom.

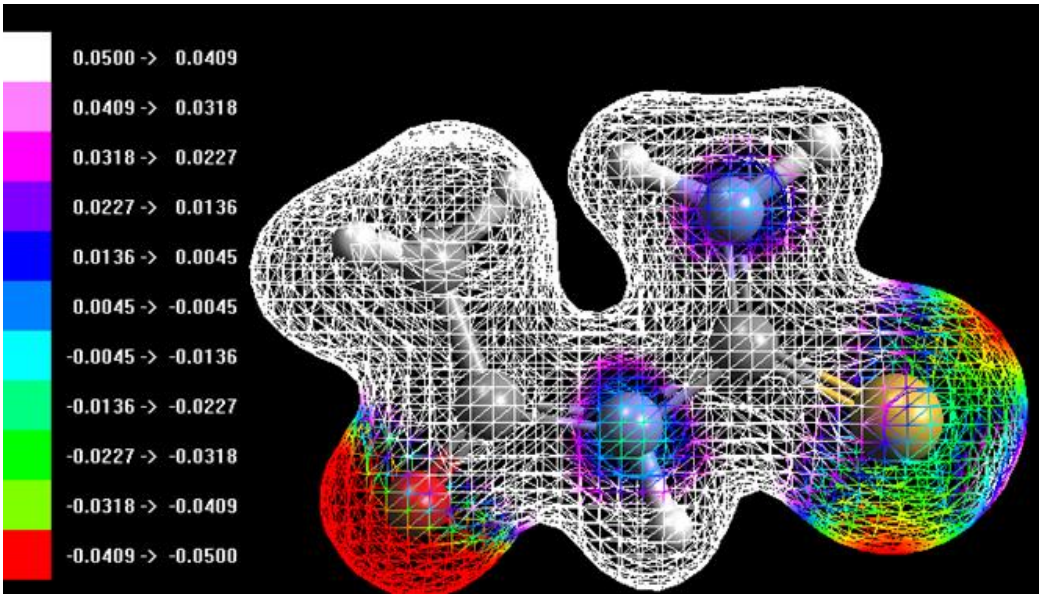


**Fig 5. Electrostatic Potential Surface Calculated at B3Lyp/6-311G(d,p)**

**Electrostatic Surface Potential Mapping**

Electrostatic Surface Potential Maps are very useful three dimensional diagrams of molecules. They enable us to visualize the charge distributors of molecules and charge related properties of molecules. They also allow us to visualize the size and shape of molecules. In organic Chemistry, Electrostatic Surface Potential Maps are invaluable in predicting the behavior of complex molecules. Red indicates the lowest Electrostatic Potential energy, and blue indicates the highest Electrostatic Potential energy. Intermediary colors presents intermediary Electrostatic Potential. The relationship between Electrostatic Potential and charge distribution. Areas of low potential, red are characterized by an abundance of electrons. Areas of high potential, blue, are characterized by a relative absence of electrons. Oxygen has a higher electronegativity vale than sulfur. Electrostatic Potential maps can also be used to determine the nature of the molecules chemical bond. There is a great of intermediary potential energy, the non-red or blue regions, in this diagram. This indicates that the electronegativity difference is not very great. In a molecule with a great electronegativity difference, charge is very polarized. And there are significant differences in electron density in different regions of the molecule. This great electronegativity difference leads to regions that the almost entirely red and almost entirely blue.

**Table 9. Condensed Fukui functions calculated by B3LYP/6-311++G(d,p) of NATU**

| Atoms | fk+ | fk- | fk0 | Sfk+ | Sfk- | Sfko | wfk+ | wfk- | wfo | fk+SFK+ | fk-Sfk- | fosfo |
|---|---|---|---|---|---|---|---|---|---|---|---|---|
| N1 | 0.3848 | -0.0189 | 0.1830 | 0.0412 | -0.0020 | 0.0196 | 1.0062 | -0.0495 | 0.4784 | 1.5842 | 0.0038 | 0.3581 |
| C2 | -0.1877 | 0.0268 | -0.0805 | -0.0201 | 0.0029 | -0.0086 | -0.4908 | 0.0701 | -0.2104 | 0.3769 | 0.0077 | 0.0692 |
| S3 | 1.0413 | 0.3899 | 0.7156 | 0.1114 | 0.0417 | 0.0765 | 2.7227 | 1.0195 | 1.8711 | 11.5986 | 1.6262 | 5.4777 |
| N4 | 0.4485 | 0.0510 | 0.2498 | 0.0480 | 0.0055 | 0.0267 | 1.1727 | 0.1334 | 0.6531 | 2.1518 | 0.0278 | 0.6673 |
| C5 | -0.3711 | 0.1383 | -0.1164 | -0.0397 | 0.0148 | -0.0125 | -0.9703 | 0.3616 | -0.3043 | 1.4732 | 0.2046 | 0.1449 |
| O6 | 0.4529 | 0.1400 | 0.2964 | 0.0485 | 0.0150 | 0.0317 | 1.1843 | 0.3660 | 0.7751 | 2.1944 | 0.2096 | 0.9400 |
| C7 | 0.4171 | -0.0161 | 0.2005 | 0.0446 | -0.0017 | 0.0214 | 1.0906 | -0.0420 | 0.5243 | 1.8610 | 0.0028 | 0.4301 |
| N1 | -0.2882 | 0.0530 | -0.1176 | -0.0308 | 0.0057 | -0.0126 | -0.7536 | 0.1386 | -0.3075 | 0.8886 | 0.0301 | 0.1479 |
| H8 | -0.2660 | 0.0536 | -0.1062 | -0.0285 | 0.0057 | -0.0114 | -0.6956 | 0.1401 | -0.2778 | 0.7570 | 0.0307 | 0.1207 |
| H9 | -0.2033 | 0.0324 | -0.0855 | -0.0217 | 0.0035 | -0.0091 | -0.5316 | 0.0846 | -0.2235 | 0.4422 | 0.0112 | 0.0782 |
| H10 | -0.1572 | 0.0804 | -0.0384 | -0.0168 | 0.0086 | -0.0041 | -0.4111 | 0.2103 | -0.1004 | 0.2644 | 0.0692 | 0.0158 |
| H11 | -0.1355 | 0.0348 | -0.0504 | -0.0145 | 0.0037 | -0.0054 | -0.3544 | 0.0910 | -0.1317 | 0.1965 | 0.0130 | 0.0271 |
| H12 | -0.1355 | 0.0348 | -0.0503 | -0.0145 | 0.0037 | -0.0054 | -0.3543 | 0.0911 | -0.1316 | 0.1965 | 0.0130 | 0.0271 |

Oxygen has a higher electron negativity values than nitrogen atoms. Oxygen atoms would consequently have a higher electron density that corresponds to a red position on it, whose value is -0.0409 to -0.05000. There are sphere shaped objects that have Blue regions. These areas correspond to the location of the nitrogen atoms ($N_1$ & $N_2$), whose value is 0.0136 – 0.0045.

**Thermodynamic properties**

On the basis of vibrational analysis and statistical Thermodynamics, the standard thermodynamic functions, heat capacity $C_p{}^o$ m entropy $S_m{}^o$ and enthalpy ($H_0{}^1$) are calculated and listed in Table 10. It can be observed that this Thermodynamic Function are increasing with temperature ranging from 100 to 800 k due to the fact that the molecular Vibrational intensities increases with Temperature. The Correlation equation between heat capacities, entropies, enthalpy changes and temperature are

$$\mathbf{C_{p,m} = 0.125\ J + 14.16\ (R^2 = 0.9963,\ SD = 2.136\ )}$$

$$\mathbf{S_m = 0.1749\ J + 69.64\ (R^2 = 0.9978,\ SD = 2.254)}$$

$$\mathbf{H_m = 0.06569\ J + 129.28\ (\ R^2 = 0.987,\ SD = 2.112\ )}$$

**Table 10. Thermodynamic properties at different temperatures at the B3LYP/6-311++G(d,p) level for NATU molecule**

| $T(K)$ | $C^o_{p,m}(cal\ mol^{-1}K^{-1})$ | $S^o_m(cal\ mol^{-1}K^{-1})$ | $\Delta H^o_m(K\ \mathrm{Cal}\ mol^{-1})$ |
|---|---|---|---|
| 100 | 274.55 | 64.45 | 4.78 |
| 200 | 328.55 | 95.84 | 12.8 |
| 298.15 | 372.58 | 124.44 | 23.63 |
| 300 | 373.35 | 124.95 | 23.87 |
| 400 | 412.88 | 150.47 | 37.67 |
| 500 | 448.84 | 171.89 | 53.82 |
| 600 | 481.78 | 189.44 | 71.92 |
| 700 | 512.1 | 203.86 | 91.61 |
| 800 | 540.13 | 215.89 | 112.61 |
| 900 | 566.17 | 226.09 | 134.72 |
| 1000 | 590.45 | 234.85 | 157.78 |

The Corresponding fitting factor ($R^2$) for these thermodynamic properties were found to be 0.9963, 0.9978, and 0.987 respectively. Standard deviation values for these Thermodynamic properties were found to be and respectively. The Temperature defence correlation graphs are shown in fig 9-11. All these thermodynamic data provide helpful information for further study on, NATU. They can be used to compute the other thermodynamic parameters, According to relationships of the functions and to determine the directions of chemical reactions according to the $2^{nd}$ law of thermodynamics [53].

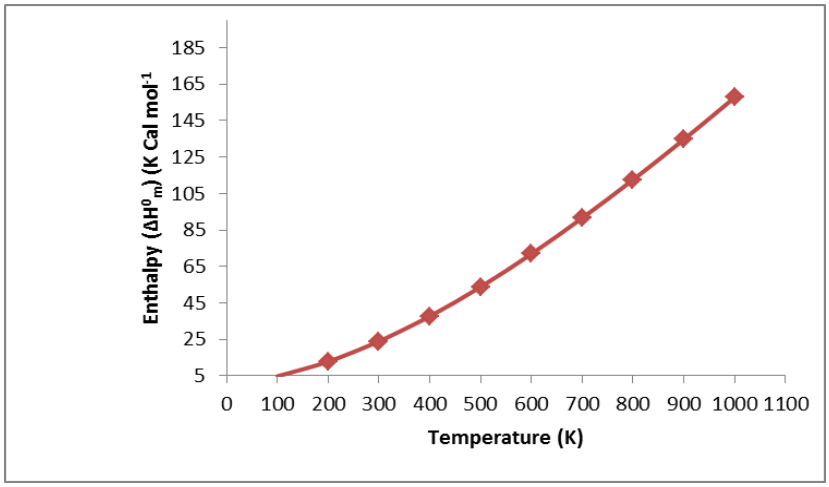


**Fig 9. Correlation Graph between Enthalpy and Temperature**

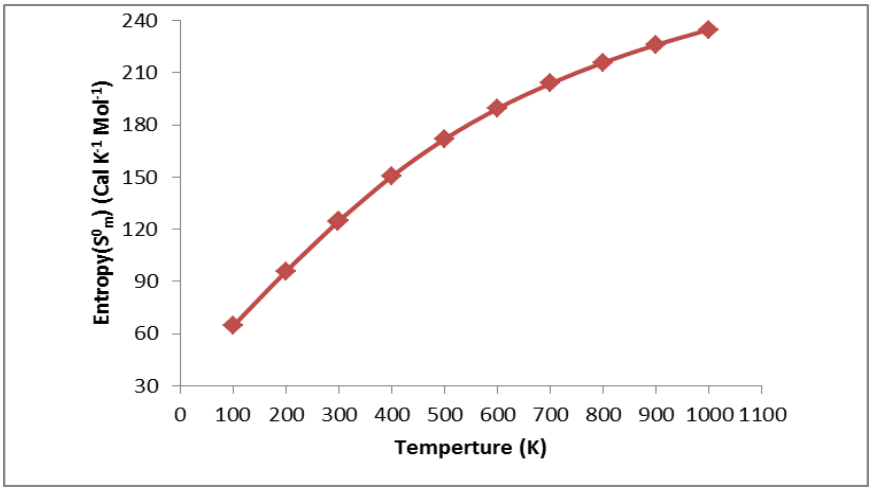


**Fig 10. Correlation Graph between Entropy and Temperature**

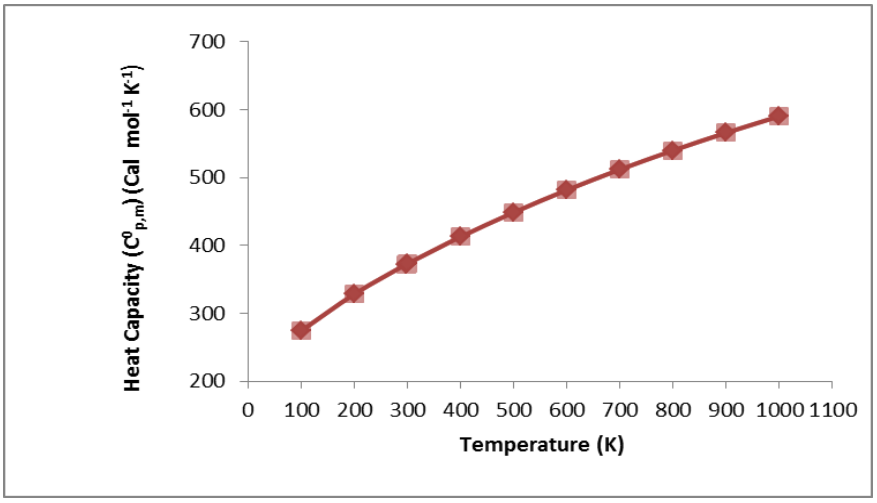


**Fig 11. Correlation Graph between Heat Capacity and Temperature**

**Conclusion of NATU**

We have carried out density functional theory calculations on the structure, vibrational spectrum, hyper polarizability, NBO, Mulliken atomic charges, Fukui function Molecular electrostatic potential, Electrostatic surface potential map, Homo-Lumo analysis and Thermodynamic properties of NATU. The equilibrium geometry by B3LYP/6.31++G (d,p), 6.311++G (d,p) level for both the bond length and bond angles is performed better. The vibrational frequency analysis by B3LYP/6.31++G(d,p), 6.311++G (d,p) method agrees satisfactorily with experimental results. On the basis of agreement between the calculated and experimental results, assignments of all the fundamental vibrational modes of NATU, are examined and proposed in this investigation. Therefore, the

assignments made at higher level of theory with higher basis set with only reasonable derivations from the experimental values. The first hyperpolarizability of the compound studied have been calculated DFT method with 6.311++G (d,p) basis set. The DFT calculated non Zero μ value of this ligand shows that the NATU Compound might have microscopic first hyper polarizability with non-Zero values obtained by the numerical second derivatives of the electric dipole moment according to the applied field strengths. The high degree of stabilization emanating from strong mesomeric effects has been well demonstrated by NBO Analysis, The NATU can lead to a variation of Mulliken charge of the whole atoms in molecules specially the atoms at and near in molecules specially the atoms at and near to the substituent.

The fukui functions is usually evaluated and interpreted from the computation of a charge of the electronic density due to the removal (addition) of one electron from to the whole molecule. The MEP shows that the negative potential sites are on nitrogen, carbon, and Hydrogen atoms, as well as the positive potential sites are around the oxygen and Sulphur atoms. These sites may provide information about the possible reaction regions for the title structure can convey information about the charge distribution of NATU Electrostatic potential energy maps similarly, the shows that oxygen has a higher electro negativity values than nitrogen atoms. The lowering of HOMO-LUMO band gap supports bioactive property of the molecule.

Furthermore, theoretical calculations give the thermodynamic properties (heat capacity entrophy, and enthalpy) for the compound. It can be observed that these thermodynamic functions are increasing with Temperature (100-700K) due to the fact that the molecular vibrational intensities increase with temperature. The present quantum chemical study may further play an important role in understanding of the structure activity and dynamic of the molecule.

**References**

[1] M. Castella-Ventura, E. Kassab, G. Buntinx,O. Poizat, Phys. Chem. Chem. Phys**. 2,** 4682 (2000).

[2] D. N. Shin, J.W. Hahn, K. H. Jung, T. K. Ha,J. Raman Spectroscope. **29**, 245 (1998).

[3] B. Giese, D. McNaughton, Phys. Chem. Chem. Phys.**4**, 5161 (2002).

[4] R. G. Parr, W. Yang, Density-Functional Theory of Atoms and Molecules, Oxford UniversityPress, New York, (1989)

[5] A. D. Becke, J. Chem. Phys. **98**, 5648 (1993).

[6] C. Lee, W. Yang, R. G. Parr, Phys. Rev**. B 37,** 785(1988).

[7] V. Chi , Chem. Phys. **300**, 1 (2004).

[8] W. Zierkiewicz, D. Michalska, B. Czarnik-Matusewicz, M. Raspenk, J. Phys. Chem. A **107**,4547 (2003).

[9] G. Korth, M. I. de Heer, P. Mulder, J. Phys. Chem.**106**, 8779 (2002).

[10] S.Nishimura, Progr. Nucl. Acid. Res. Mol. Biol., **12**,50 (1972).

[11] B.G.Barrell and B.F.C.Clark, Handbook of nucleic acid sequences,Oxford: Joynson-Brunuvers.(1974).

[12] M.Ya.Feldman, Progr. Biophys. Mol. Biol., **32**, 83 (1977).

[13] M.A.Ali and S.E.Livingstone, Coord. Chem. Rev., **13**, 101 (1974).

[14] K.Geetharani and D.N.Sathyanarayana, Spectrochim Acta, **32A**, 227 (1976).

[15] Y.Saito and K.Machida, Spectrochim. Acta, **35A,** 369 (1979).

[16] M.J. Frisch, G.W. Trucks, H.B. Schlegel, G.E. Suzerain, M.A. Robb, J.R. Cheeseman, Jr., J.A. Montgomery, T. Vreven, K.N. Kudin, J.C. Burant, J.M. Millam, S.S. Iyengar, J. Tomasi, V. Barone, B. Mennucci, M. Cossi, G. Scalmani, N. Rega, G.A. Petersson, H. Nakatsuji, M. Hada, M. Ehara, K. Toyota, R. Fukuda, J. Hasegawa, M. Ishida, T. Nakajima, Y. Honda, O. Kitao, H. Nakai, M. Klene, X. Li, J.E. Knox, H.P. Hratchian, J.B. Cross, V. Bakken, C. Adamo, J. Jaramillo, R. Gomperts, R.E. Stratmann, O. Yazyev, A.J. Austin, R. Cammi, C. Pomelli, J.W. Ochterski, P.Y. Ayala, K. Morokuma, G.A. Voth, P. Salvador, J.J. Dannenberg, V.G. Zakrzewski, S. Dapprich, A.D. Daniels, M.C. Strain, O. Farkas, D.K. Malick, A.D. Rabuck, K. Raghavachari, J.B. Foresman, J.V. Ortiz, Q. Cui, A.G. Baboul, S. Clifford, J. Cioslowski, B. Stefanov, G. Liu, A. Liashenko, P. Piskorz, I. Komaromi, R.L. Martin, D.J. Fox, T. Keith, M.A. Al-Laham, C.Y. Peng, A. Nanayakkara, M. Challacombe, P.M.W. Gill, B. Johnson, W. Chen, M.W. Wong, C. Gonzalez, and J.A. Pople, Gaussian 03, Revision A.I, Gaussian, Inc, Pittsburgh, PA, 2003.

[17] P. Pulay, G. Fogarasi, G. Pongor, J.E. Boggs, A. Vargha, J. Am. Chem. Soc. **105** 7037–7047 (1983).

[18] G. Rauhut, P. Pulay, J. Phys. Chem. **99** 3093–3100 (1995).

[19] T. Sundius, J. Mol. Struct. **218**, 321–326(1990)

[20] T. Sundius, Vib. Spectrosc. **29** , 89–95 (2002)

[21] G. Keresztury, S. Holly, J. Varga, G. Besenyei, A.Y. Wang, J.R. Durig, Spectrochim. Acta A 49 (1993) 2007–2026.

[22] G. Keresztury, in: J.M. Chalmers, P.R. Griffith (Eds.), Raman Spectroscopy: Theory in Handbook of Vibrational Spectroscopy, vol. 1, John Wiley & Sons Ltd.,New York, 2002.

[23] E. B. Wilson, Jr., J. C. Decius, and P. C. Cross, Molecular Vibrations (McGraw-Hill, New York (1955)

[24] W. J. Orville-Thomas, J. Chem. Phys**. 19** 1162 (1951).

[25] Y. Morino and K. Kuchitsu, J. Chem. Phys. **20** 1809 (1952).

[26] P.Hohenberg, W. Kohn, *Phys. Rev. B* **136**, 864 (1964).

[27] R.G. Parr, W. Yang ,J.Am. Chem. Soc . **105**, 7512 (1983)

[28] R.G. Parr, W. Yang ,J.Am. Chem. Soc . **106**, 4049 (1984)

[29] R.G. Parr, W. Yang Proc. Natl.Acad. Sci. U.S.A. 821, 6723 (1985)

[30] J.L. Gazquez,, F. Mendez. J. Phys. Chem**., 98**, 4591 (1994)

[31] J.L. Gazquez,, F. Mendez. J. Phys. Chem**., 97**, 4059 (1993)

[32] D.Keresztuny and M.P.Marzochi, Spectrochim. Acta, **31A**, 275 (1975).

[33] D.N.Sathyanarayana, K.Volka and K.Geetharani, Spectrochim. Acta, **33A**, 517 (1977).

[34] K.Dwarakanath and D.N.Sathyanarayana, Bull. Chem.Soc., Japan **52** 2084 (1979)

[35] R.K.Ritchie, H.Speeding and D.Steele, Spectrochim Acta, **27A**,1597 (1971)

[36] K.R Gayathri Devi and D.N.Sathyanarayana Bull.Chem.Soc. Japan,**53**, 2990 (1980)

[37] T.Suzuki, Bull Chem. Soc. Japan **35,** 1286, 1449 (1962)

[38] W.Walter and P.Staglich, Spectrochim Acta **30A** 1739 (1994)

[39] K.Geetharani and D.N.Sathyanarayana, Spectrochim Acta, **32A**, 227 (1976)

[40] J.P. Foster, F. Weinhold, J. Am. Chem. Soc. 102 7211–7218 (1980)

[41] M. Snehalatha, C. Ravi kumar, I. Hubert Joe, N. Sekar, V.S. Jayakumar, Spectrochim. Acta 72A 654,2009

[42] C.R. Zhang, H.S. Chen, G.H. Wang, Chem. Res. Chin. U 20 640–646.(2004)

[43] Y. Sun, X. Chen, L. Sun, X. Guo, W. Lu, Chem. Phys. Lett. 381 397–403, (2003)

[44] O. Christiansen, J. Gauss, J.F. Stanton, Chem. Phys. Lett. 305, 147–155.(1999)

[45] D.A. Kleinman, Phys. Rev. 126 1977 (1962)

[46] G. Keresztury, in: J.M. Chalmers, P.R. Griffiths (Eds.,) Raman Spectroscopy; Theory, Handbook of Vibrational Spectroscopy. John Wiley and Sons Ltd., 1 7 (2002)

[47] M. Arivazhagan, K. Sampathkumar & S. Jeyavijayan, Indian J Pure & Appl. Phys, 48 716 (2010)

[48] I. Sidir, Y.G. Sidir, M. Kumalar, E. Tasal, J. Mol. Struct. 964 ,134.(2010)

[49] P. Kolandaivel, G. Praveen, and P. Selvarengan, J. Chem.Sci. 117(5) 591–598 (2005).

[50] R.K. Roy, K. Hirao, S. Krishnamurthy, and S. Pal, J. Chem. Phys. 115, 2901–2907 (2001)

[51] E. Scrocco, J. Tomasi, Adv. Quantum Chem. 11.(1979)

[52] N. Okulik, A.H. Jubert, Internet Electron J. Mol. Des. 4 (2005)

[53] R. Zhang, B. Dub, G. Sun, Y. Sun, Spectrochim. Acta A 75 1115, 2010.